

MODELLING OF BUBBLE BREAK-UP IN STIRRED TANKS

by

Goran ŽIVKOVIĆ and Stevan NEMODA

Original scientific paper
UDC: 532.517.4:519.876.5
BIBLID: 0354-9836, 8 (2004), 1, 29-49

The Lagrangian code LAG3D for dispersed phase flow modeling was implemented with the introduction of bubble break-up model. The research was restricted on bubbles with diameter less than 2 mm, i. e. bubbles which could be treated as spheres. The model was developed according to the approach of Martinez-Bazan model. It was rearranged and adjusted for the use in the particular problem of flow in stirred tanks. Developed model is stochastic one, based on the assumption that shear in the flow induces the break of the bubble. As a dominant parameter a dissipation of the turbulent kinetic energy was used.

Computations were performed for two different types of the stirrer: Rushton turbine, and Pitch blade turbine. The geometry of the tank was kept constant (four blades). Two different types of liquids with very big difference in viscosity were used, i. e. silicon oil and dimethylsulfoxide, in order to enable computation of the flow in turbulent regime as well. As a parameter of the flow, the number of rotations of the stirrer was varying. As a result of the computation the fields of velocity of both phases were got, as well as the fields of bubble concentration, bubble mean diameter and bubble Sauter diameter.

To estimate the influence of the break-up model on the processes in the stirred tank a computations with and without this model were performed and compared. A considerable differences were found not only in the field of bubble diameter, but also in the field of bubble concentration. That confirmed a necessity of the introduction of such model.

A comparison with the experiments performed with phase Doppler anemometry technique showed very good agreement in velocity and concentration profiles of the gas phase. The results for the average bubble diameter are qualitatively the same, but in almost all computations about 20% smaller bubble diameter was got than in the measurements.

Key words: *multiphase flow, turbulence, bubbles, break-up, stirred tank, model, experiment*

Introduction

Flows with a continuous liquid phase and a dispersed gas and/or solid phase are found widely spread in process engineering. Examples for applications are mineral oil conveying and processing, where the oil contains dispersed water drops, gas bubbles and solid particles, biochemical processes with flocculation materials floated by bubbles, and gas-liquid reactions with participation of a solid particulate catalyst.

Flows with a dispersed phase in a continuum are influenced by the interaction between the phases. Contrary to the continuous phase where information about local characteristics of the fluid is transported by the molecular interaction through pressure waves and diffusion, in the dispersed phase there is no analogy for the fluid pressure, and information is transported between bubbles or particles through the conveying fluid. Due to their different histories, there are local differences between hydrodynamic properties of bubbles and solid particles, which is not the case for the continuous phase. There are also phenomena in the dispersed phase with the characteristics of diffusion, caused mainly by the turbulent fluctuations in the continuous phase.

Mathematical treatment of multidimensional multiphase flows for simulating these phenomena is complicated and not yet solved. The exact approach for modelling convection and diffusion processes in multiphase flows requires the knowledge of turbulent characteristics as fluctuation velocity components, autocorrelation functions and Lagrangian integral scales of turbulence. These characteristics are not known for multiphase flows even in the simplest cases. That is why the only possible practical approach is to develop physical and mathematical models, closing the problem by using assumptions on the characteristics of the involved phenomena, or by introducing empirical correlations. Enhanced physical knowledge is required to develop improved multiphase models. It is a big challenge to overcome the closure problems between the flow equations of the different phases. Many details about forces on the phases and their interaction are still unknown. There is also a lack of knowledge about the influence of the dispersed phases on the turbulent velocity fluctuations in the continuous phase which is necessary for improving turbulence models. For modelling the dispersed phase, either the Eulerian or the Lagrangian approach can be used. The Eulerian approach treats the dispersed phase like a fluid. Its main advantage is that it is less time consuming on the computer than the Lagrangian approach. An example of successful two-phase flow modelling by the Eulerian approach is the work of Mostafa and Elghobashi ⁹. The Lagrangian approach is closer to the physical reality and yields information necessary for an accurate prediction of particle motion in the turbulent field. For this reason it has been chosen for the present work.

The theoretical basis for phase interaction was established by Migdal and Agosta ⁷. According to their model, solid particles, drops and bubbles are treated as sources of mass, momentum and energy in the fluid, represented by source terms in the equations of change. Crowe *et al.* ³ used this idea to develop the Particle-Source-in-Cell (PSI-CELL) model. In many models developed later, special attention was given to some particular phenomena in multiphase flows. Rubinow and Keller ¹¹ developed a theoretical expression for the lift force which acts on a sphere rotating

in a viscous fluid. Saffman¹² modelled the motion of a sphere near the wall, where the influence of the fluid velocity gradient on the sphere motion was taken into account. Matsumoto and Saito⁶ modelled particle-wall collisions and investigated the role of wall roughness in preventing particle sedimentation. Wall roughness was modelled by a periodic sinusoidal function, with its amplitude representing the roughness height. Particle non-sphericity was accounted for by treating the particles as ellipsoids. Tsuji *et al.*¹⁵ developed a two-phase model for the flow through a horizontal tube, taking into account the Magnus lift force. Milojević⁸ modelled the effect of fluid turbulence on the dispersed phase, taking into account the crossing-trajectories effect. Sommerfeld and Živković¹⁴ similar to Oesterle and Petitjean¹⁰ developed a model in which they simulated wall roughness by the stochastic change of the wall inclination in the model. They also developed a model for particle-particle collisions. The collisions were regarded as a stochastic event, similar to collisions between gas molecules, which can be described by the kinetic theory of gases.

In order to simulate realistic flow of mixture of water with air bubbles Martinez-Bazan *et al.*^{4, 5} developed a statistical model of bubble break-up induced by the turbulence shear stresses. It showed very good agreement with experiments, and therefore its basic principles was taken as the basis of the presented model.

There is no doubt that stirred tanks play an extraordinary important role in modern industry. For example, according to some estimation about half of the annual output of the US chemical industry is at some stage of production circulated through stirred-tank reactors. This fact imposes the necessity of taking a special care in modelling processes in them. The change of the geometry of the flow domain due to the rotation of stirrer relative to the solid walls is characteristic which distinguishes flow in stirred tanks from the other types of flows usually met in process engineering. This asks for the special approach in the numerical modelling of such types of flows. There exists a direct, unsteady approach, *clicking grids*, which was found to be extremely time consuming and not convenient for the case of two-phase flow computations. The problem was solved by introducing *Multiple-Frame-of-Reference*. According to this approach the inner part of the flow field which comprehends the stirrer is rotating, which was simulated by introducing the additional terms in the partial differential equations which describe the flow in that domain. These terms simulate centrifugal and coriolis forces. In the other part of the flow field everything stays the same. With this approach the relative motion of the blades to the baffles were neglected, according to the assumption the relative position of the blades can not influence significantly the field close to the baffles and that fluid close to the blades do not “feel” the existence of blades. The border between the rotating and non-rotating parts was of course chosen to be far enough from both baffles and blades. Wechsler *et al.*¹⁶ have shown that there is no significant difference in results of both mentioned approaches, vindicating the use of *Multiple-Frame-of-Reference* method.

This work is a result of the striving to simulate numerically processes in stirred tanks in their full complexity. Since the gas-liquid mixture occurs very often in various mixing processes, where bubble break-up is either a side effect of the mixing process or even its main target, it is inevitable to include a bubble break-up model in any realistic numerical description of the mixing process.

The following section describes the main features of the adopted two phase-flow numerical code and developed break-up model. Section three presents the computed results and the comparisons of experimental and numerical results. Finally, conclusions from the work are drawn.

Model of dispersed phase flow

As the basis for the modelling of the gas phase the LAG3D code for the computation of the two-phase gas-particle flow was used. It was developed under the supervision of Prof. Martin Sommerfeld, first at the Chair of Fluid Mechanics at the Friedrich Alexander University, Erlangen-Nuremberg, Germany, and then at the Chair of Mechanical Process Engineering at the Martin Luther University of Halle-Wittenberg, Germany. The basic characteristics of the code were: (1) Lagrangian approach; (2) Particles or bubbles are treated as ideal spheres; (3) All relevant forces included; (4) Particle-wall interaction included; (5) Particle-particle interaction included; (6) Langevin's model of particle-fluid turbulent eddy interaction. In order to extend the use of the code on gas-liquid problems it was necessary to add added mass force in the equations of bubble motion. A detailed survey of the model could be found in [2, 14].

LAG3D code was originally developed only for the solid dispersed phase, which represented its domain of application. True, it was already implemented with some additional elements, like added mass force, which could allow the use of the model in other types of multiphase flows, as are flows with bubbles as one of the phases. Such model could be successfully applied for all types of flow where the bubbles are relatively small (say less than 1 mm) and the flow is either laminar or the level of turbulence is small, *i. e.* where bubbles break-up rarely. This is not the case for the flows in stirred tanks. The flow in stirred tanks is in most cases characterized with the high level of shear stresses, which act on bubbles and induce their frequent break-up. This is especially characteristic for the regions of the stirred tank close to the stirrer. Experiments showed that for relatively low number of rotations of the stirrer of 500-600 rot./min. the bubbles which enter the tank with the relatively small diameter of about 1.5 mm break-up in average at least few times, reaching the final value of about 0.4 mm.

This shows that for the successful simulation of the processes in stirred tanks the LAG3D model should be additionally implemented with the model of bubbles break-up. Of course, the model should be general enough to enable its application in the other devices as well. Bubble coalescence can play an important role also, but only in cases of large gas hold up, like in real industrial cases (10% and more). The sphericity of the particles (in this case bubbles) remained as the basic assumption of the model, which restricted the use of the model to air bubbles less than 2 mm. In the experiments performed to verify the model at the entrance of the stirred tank bubbles had diameter of about 1.7 mm and therefore small enough to vindicate the assumption.

As the basis for the developed model the Martinez-Bazan approach [4, 5], developed at San Diego University, US, was taken. This is a statistical approach in which the break-up of the bubble and the diameters of daughter bubbles are stochastic events.

This means that one could only estimate the probability that some particular bubble will brake in a given portion of time. Also, instead of knowing the exact diameters of the daughter bubbles only their probability density function (p.d.f.) could be calculated. Nevertheless, applying this knowledge on the large sample of bubbles (in any real process the sample of bubbles in some stirred tank is inevitably enormous) using such approach a very precise statistical description of the mixture properties could be achieved.

The basic assumptions of this model were adopted in the presented model too. According to it:

- (1) For bubbles to break-up, its surface has to deform and deformation is provided by the turbulent stresses generated in the surrounding liquid. This assumption is in accordance with already mentioned fact of the importance of the role of the turbulent and shear stresses in stirring and mixing processes;
- (2) Probability of the bubble splitting should be weighted with the difference between turbulent stresses and surface restoring pressure.

As the result of the break-up modelling one gets: (1) bubble splitting frequency; (2) number of daughter bubbles, and (3) p.d.f. function of daughter bubbles diameters.

Bubble break-up model

A minimum energy E_s to deform the bubble of the diameter D_0 could be connected with the bubble surface tension σ :

$$E_s = \pi\sigma D_0^2 \quad (1)$$

From this one obtains the surface restoring tension:

$$\tau_s = \frac{6E_s}{\pi D_0^3} = \frac{6\sigma}{D_0} \quad (2)$$

In the model bubble represents a sphere of finite size submerged in the turbulent field of the surrounding liquid. Therefore, due to the turbulent fluctuations of the liquid velocity, at the same instant the fluid velocity at different points of the sphere would differ, resulting in the overall turbulent stress which acts on the sphere. This turbulent stress can be connected with the mean squared velocity difference on the two points on the bubble:

$$\tau_t = \frac{1}{2} \rho \overline{\Delta u^2} \quad (3)$$

where

$$\overline{u^2} = \overline{|u(x, D_0, t) - u(x, t)|^2} = \beta(\varepsilon, D_0)^{2/3} \quad (4)$$

ε represents the dissipation of turbulent kinetic energy, and β represents the Batchelor constant. From [1] it was taken that $\beta = 8.2$.

In order that bubble brakes it is necessary that $\tau_t > \tau_s$. This criteria determines the critical diameter. The diameter of the bubble should be bigger than it in order for bubble to brake. Using eqs. (2), (3), and (4):

$$D_c = \frac{12\sigma}{\beta\rho} \varepsilon^{2/5} \tag{5}$$

The condition that $D_0 > D_c$ is not sufficient. Bubble will break-up only if the distance between the positions of turbulent fluctuations on the bubble surface which tend to brake it up is bigger than some minimal value L_{\min} . To calculate this value one should equate the restoring surface force (surface tension) τ_s given in eq. (2) with the deformation surface force τ_t given in eq. (3), where the bubble diameter D_0 is replaced by L_{\min} :

$$\frac{1}{2} \rho \beta (\varepsilon L_{\min})^{2/3} = 6 \frac{\sigma}{D_0} L_{\min} = \frac{12\sigma}{\beta\rho D_0} \varepsilon^{3/2} = \frac{D_c^{5/3} \varepsilon^{2/3}}{D_0} \varepsilon^{3/2} = \frac{D_c^{5/2}}{D_0^{3/2}} \tag{6}$$

From eq. (6) it is obvious that with the increase of D_0 the value of L_{\min} decreases, which shows that bigger bubbles are more unstable than smaller ones and that break-up more easily.

It was assumed in [4] that the rate at which the break-up process takes place is inversely proportional to the difference between the deformation and restoring forces. According to this assumption which looks acceptable at least as the first approximation in the description of the break-up process, the break-up time t_b is proportional to:

$$t_b = \frac{D_0}{\sqrt{u^2 - \frac{12\sigma}{\rho D_0}}} \tag{7}$$

The break-up frequency is then given by:

$$g = t_b^{-1} = K_g \frac{\sqrt{\Delta u^2 - \frac{12\sigma}{\rho D_0}}}{D_0} = K_g \frac{\sqrt{\beta(\varepsilon D)^{2/3} - \frac{12\sigma}{\rho D_0}}}{D_0} \tag{8}$$

where K_g represents the constant whose value was experimentally determined in [5] to be $K_g = 0.25$.

The good characteristic of the model is that there exists the value of bubble diameter for which the break-up frequency reaches its maximal value, which is in accordance with the experiments. On this way, the same model could be applied to the wide range sizes of the bubble diameter.

The next assumption is that in the break-up process the mother bubble breaks only on two daughter bubbles. This assumption simplifies the modelling of the break-up process excluding complicated cases in which in the given portion of time a particular bubble breaks on several daughter bubbles. On the other hand it is quite acceptable, for

any breaking process which gives more than two daughter bubbles could be resolved on few different processes (which give as the result of breaking only two daughter bubbles) simply by reducing the time step Δt (the above mentioned portion of time) between the two calculated instants.

We finally come to the problem of the determination of size of the daughter bubbles. They clearly depend on the intensity of the turbulent stresses and the position on the bubble surface where they act. The fact that in principle they could act at any point on the bubble surface gives the problem a three-dimensional character (beside its obvious stochastic character). Still, the model could be simplified with the assumption that at the given time step Δt two turbulent fluctuations (stresses) act on the bubble. Let us denote a distance between their acting points with L . The maximal value of this distance is of course bubble diameter. If these stresses overcome a surface tension of the bubble it will break. The crucial question now is where the brake will take place? It is logical to assume that only a part of the bubble “between” the points in which the turbulent stresses act are really under the tension as the outcome of their action, and that the rest of the bubble remains uninfluenced. (Such consideration has something one-dimensional in nature, since it is very hard to define rigorously what does that mean “between” the two points on the sphere. Still, authors believe that such simplification should not influence the accuracy of the bubble break-up description with the proposed model. The final evaluation can of course be performed through the comparison of the calculated results with the experiments.) It is then logically to assume that this part of the bubble which is subjected to the turbulent stresses would split on two equal parts. Still, one of these parts is attached to the rest of the bubble. Consequently, the mother bubble will split on two unequal daughter bubbles, where the volume of the smaller one will be one half of the volume of the part of the mother bubble which was subjected to turbulent stresses.

As the eq. (4) shows, with the increase of the distance of the acting points the turbulent stress increases. The model has to correlate somehow this increase of the surface tension, *i. e.* the difference $\tau_t - \tau_s$ with the distance L . As the simplest and the most straightforward a linear dependence was assumed. If with $P(L)$ we denote the probability density function that the break-up will happen when the acting points of the turbulent stresses are at distance L :

$$L \geq L_{\min} \quad P(L) = 0 \quad (9a)$$

$$L \geq L_{\min} \quad P(L) = \frac{1}{2} \rho \beta (\varepsilon L)^{2/3} \frac{6\sigma}{D_0} \quad (9b)$$

According to the proposed model the value L represents the diameter of the part of the mother bubble which splits on two halves. Let us denote a diameter of one of these halves (which represents, as explained above a smaller of two daughter bubbles) with D_s . Then:

$$D_s = \frac{1}{2} L^{3/4} \quad (10)$$

Inserting the eq. (10) in the eq. (9) we get:

$$D_s = \frac{1}{2^{1/3}} L_{\min} P(D_s) = 0 \quad (11a)$$

$$D_s = \frac{1}{2^{1/3}} L_{\min} P(D_s) = \frac{1}{2^{7/9}} \rho\beta(\varepsilon D_s)^{2/3} \frac{6}{D_0} \quad (11b)$$

To get the exact $P(D_s)$ dependence, eq. (11b) should be normalized. It is also more convenient to represent it in non-dimensional form, in order to generalize it for any set of flow parameters. Taking the term $(1/2)\rho\beta(\varepsilon D_0)^{2/3}$ out of the brackets, one gets:

$$P(D_s) = \frac{1}{2} \rho\beta(\varepsilon D_0)^{2/3} 2^{2/9} \frac{D_s}{D_0} \frac{12\sigma}{\rho\beta\varepsilon^{2/3} D_0^{5/3}} = \frac{1}{2} \rho\beta(\varepsilon D_0)^{2/3} 2^{2/9} D^{*2/3} \frac{D_c}{D_0} \quad (12)$$

Here, with D^* we denoted the non-dimensional diameter D_s/D_0 . From the condition $P(D^*) = 0$ we get that the minimal value for D^* is:

$$D_{\min}^* = \frac{1}{2^{1/3}} \frac{D_c}{D_0} \quad (13)$$

Taking into account that D_s is a diameter of the smaller daughter bubble whose volume can not be bigger than half of the volume of the original bubble we conclude that $D_{\max}^* = 1/2^{1/3}$.

From the condition that $\int P(D^*) = 1$ one gets the final expression for $P(D^*)$ in non-dimensional form, which all parameters of flow, liquid characteristics and bubble size are represented with the single non-dimensional parameter D_c/D_0 :

$$P(D^*) = \frac{\frac{1}{2} \rho\beta(\varepsilon D_0)^{2/3} 2^{2/9} D^{*2/3} \frac{D_c}{D_0}}{\int_{D_{\min}^*}^{D_{\max}^*} \frac{1}{2} \rho\beta(\varepsilon D_0)^{2/3} 2^{2/9} D^{*2/3} \frac{D_c}{D_0} dD^*} = \frac{2^{1/3} 2^{2/9} D^{*2/3} \frac{D_c}{D_0}}{\frac{2}{5} \frac{D_c}{D_0} \frac{25/6}{D_0} \frac{D_c}{D_0} \frac{5/3}{5}} \quad (14)$$

The diameter D_b of the bigger daughter bubble is now simply calculated from:

$$D_b = D_0(1 - D^{*3})^{1/3} \quad (15)$$

On fig. 1 the shape of $P(D^*)$ for $D_c/D_0 = 0.5$ is drawn. It is not normalized to 1 in order to make a comparison with the curve presented in 5 . Both models give qualitatively the same shape of p.d.f. Nevertheless, the presented model enables that in the process of splitting one can obtain bubbles of smaller sizes than in the model of Martin-Bazan, which is in accordance with the experiments. Besides, the Martin-Bazan model suffers from one inconsistency. Namely, in this it was assumed that L_{\min} represents the value of the smallest bubble possible bubble size which appears in $P(D^*)$ distribution. If this is so, then $2D_{\min}^3 = D_0^3$. Taking into account the eq. (6):

$$2 \frac{D_c^{15/2}}{D_0^{9/2}} = D_0^3 = D_0 \cdot 2^{2/15} D_c \quad (16)$$

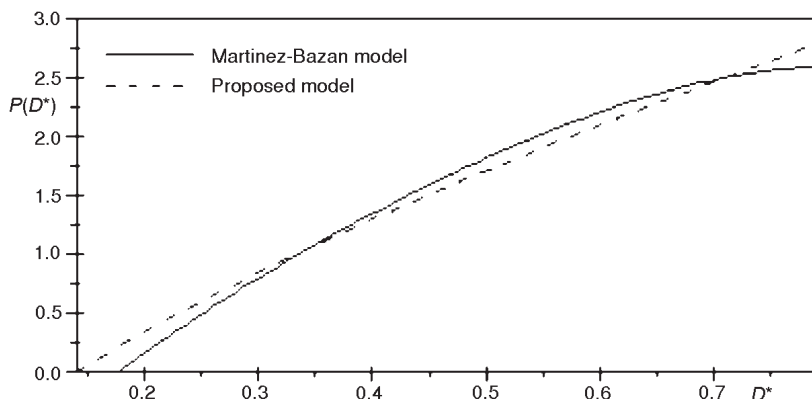


Figure 1.

That is, the diameter of the smallest bubble which can break-up is not D_c as it should be by definition, but somewhat bigger. In the presented model the smallest value for D_0 when break-up happens is exactly D_c .

The algorithm of the use of the presented break-up model is following:

- (1) From the computed field of turbulent energy dissipation using linear interpolation calculate its value at the point where the bubble is positioned at the given instant;
- (2) From (8) compute the bubble break-up frequency;
- (3) On the basis of the calculated break-up frequency and the value of the time step Δt at the given instant, using a uniform random number generator determine whether in the given Δt the break-up of the bubble will happen or not;

- (4) If not, pass to the next time step; if it happens generate random number with the p.d.f. given by eq. (14) to determine the size of the smaller daughter bubble;
- (5) From eq. (15) calculate the size of the bigger daughter bubble;
- (6) Pass to the next time step and continue to follow both daughter bubbles independently.

Computation of flow in stirred tank

Liquid phase

For the computation of the liquid phase a FASTEST-3D numerical code developed at the Chair of Fluid Mechanics at the Friedrich Alexander University was used. Rotation of the stirrer was simulated using *Multiple-Frame-of-Reference* method described in introduction. After getting the fields of liquid velocity, k and ε , a LAG3D code was used for bubble tracking. Computation was performed for two different types of stirrer: Rushton turbine with six blades and 45° Pitch blade turbine, settled at the same stirred tank, equipped with four symmetrically positioned baffles, fig 2.

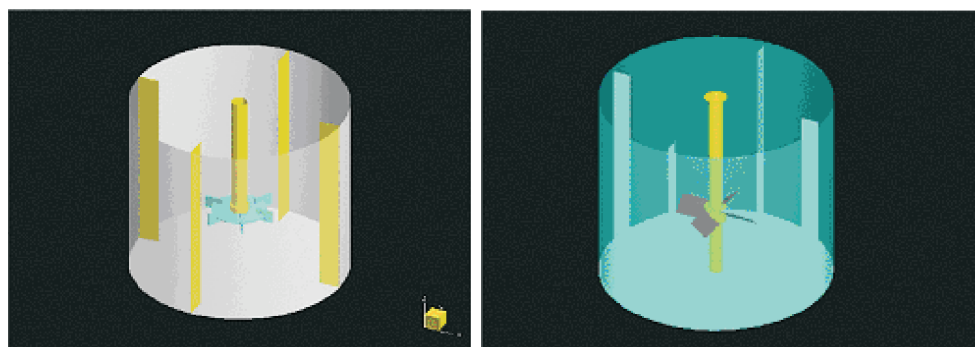


Figure 2. The geometry of stirred tank with Rushton (left) and 45° Pitch blade turbine (right)

Cylindrical tank had diameter $T = 0.152$ m with a liquid height of $H = T$, and width of the baffles $B = 0.1 T$. The thickness of baffles and stirrer blades were neglected. In both cases stirrers were placed one third of the liquid height from the bottom of the tank. Geometry of the stirrers are given in fig. 3. The cylindrical region computed in a rotating frame of reference was confined by a radial distance of 0.046 m and was located between the axial positions of 0.035 m and 0.065 m. Numerical grid had about 270,000 nodes.

The geometries as well as liquids used in computations correspond exactly to those for which the experiments were performed. Two different types of liquid were used in computation: silicon oil (Pitch blade) and dimethylsulfoxide (DMSO), (Rushton

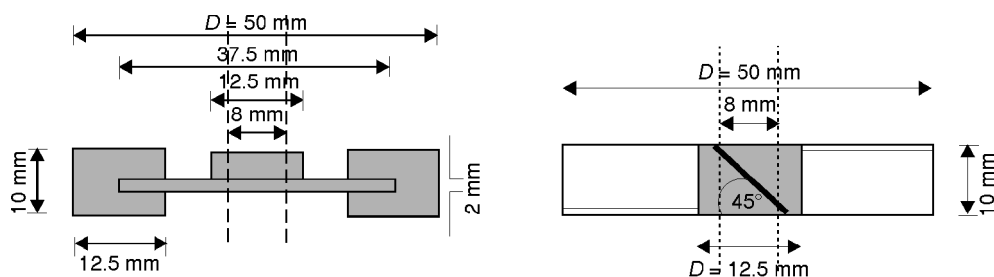


Figure 3. Geometries of the Rushton turbine (left) and Pitch blade turbine (right)

turbine). These liquids had to be used instead of water in experiments, performed with phase Doppler anemometry (PDA) technique, because both of them have the same refractive index as glass (from which a stirred tank was made), the property necessary to enable the use of PDA technique. Silicon oil has many properties very similar to water, but much bigger dynamic viscosity of 0.0159 Pa·s. With such big viscosity and usual rotational velocity of the stirrer only laminar types of flow could be achieved in the stirrer (high rotational velocity of the stirrer is not possible due to the air entrainment on the top surface near the shaft). With DMSO this problem could be overcome, since it has the viscosity very similar to water, but it is so aggressive that its use leads to enormous difficulties in performing the experiments.

The computations with DMSO as a liquid were performed for the tank with Rushton turbine, for the rotational speeds 600 and 850 rot./min. This corresponds to the Reynolds numbers of 12,850 and 18,200, respectively. In the computations with pitch blade turbine the two different directions of turbine rotations were studied. Due to the dependence of the flow pattern on the rotational direction in one case upstream, and in the other downstream recirculation zone was obtained. Both types of flow could be met in practice. The basic difference is that in the case of two phase bubble-liquid flow the residence time of the bubbles in the opened tank is much higher in the case of downstream recirculation zone. The computation was performed for silicon oil, for rotational speed of 850 rot./min., *i. e.* $Re = 2270$.

The fields of axial velocity component in the vertical cross-section which were presented on fig. 4 (Rushton) and fig. 5 (Pitch blade). In the case of the geometry with the Rushton turbine one sees clearly two recirculation zones, one above and the other below the stirrer, with fluid circulating in the opposite directions. In the case of Pitch blade turbine there is only one big recirculation zone.

The fields of turbulent kinetic energy profiles for the same cross-sections were presented on fig. 6 (Rushton) and fig. 7 (Pitch blade). In the break-up model turbulent fluctuations cause break-up of a bubble. Therefore, these profiles indicate the regions in the stirred tank where, due to the break-up model, the bubble break-up is most intensive. Due to the higher Reynolds number in the case of Rushton turbine the higher values of turbulent kinetic energy was got than in the case of Pitch blade. On the other hand,

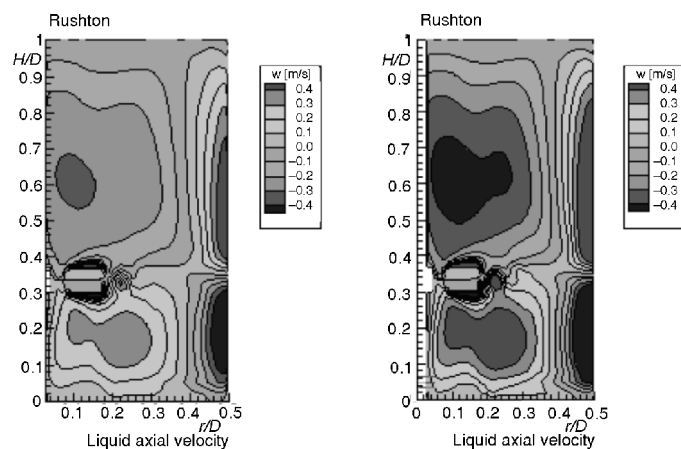


Figure 4. Axial velocity field in vertical cross section for Rushton turbine, $n = 600$ rot./min. (left) and $n = 850$ rot./min. (right) (DMSO)

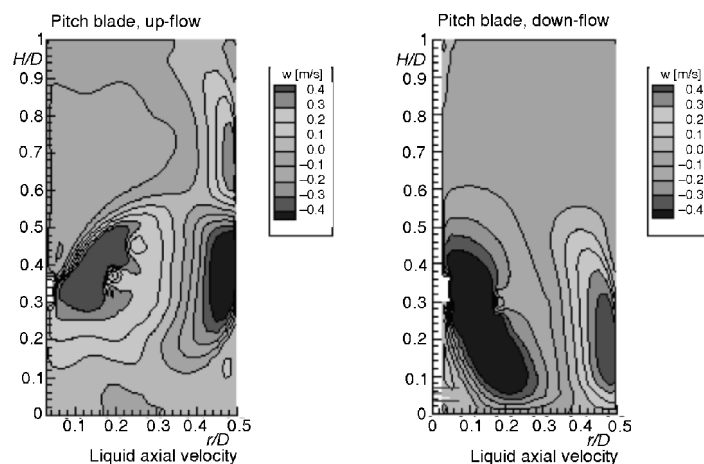


Figure 5. Axial velocity field in vertical cross section for Pitch blade turbine, $n = 850$ rot./min. (silicon oil)

in the case of Pitch blade the region of the flow field where the turbulent kinetic energy is most intensive is much wider. This is in complete agreement with the measurements of Schäfer 13 made for the $Re = 7300$. On the other hand, for the same Reynolds number Rushton turbine gives somewhat higher value of biggest turbulent kinetic energy. The wider zone of high turbulent energy means the higher probability of a bubble to pass through it and to brake. This indicates that in the processes in which the bubble break-up

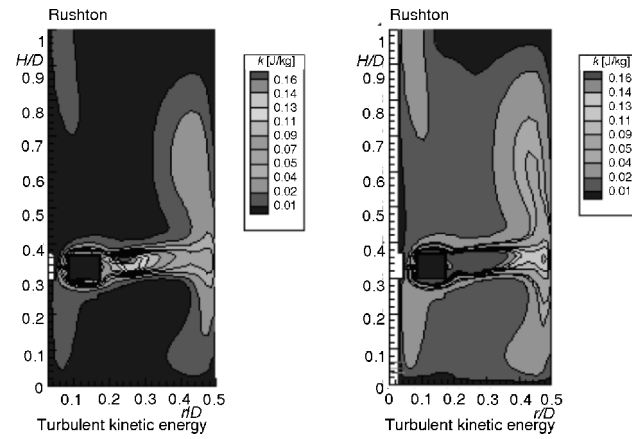


Figure 6. Turbulent kinetic energy field in vertical cross section for Rushton turbine, $n = 600$ rot./min. (left) and $n = 850$ rot./min. (right), (DMSO)

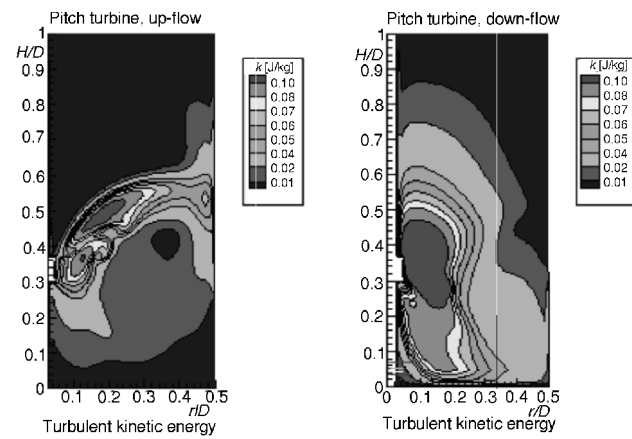


Figure 7. Turbulent kinetic energy field in vertical cross section for Pitch blade turbine, $n = 850$ rot./min. (silicon oil)

is desirable, one should use Pitch blade turbine (under the assumption that the turbulent kinetic energy intensity is high enough to brake the bubble), and in which it is not, Rushton turbine is more convenient.

Discrete gas phase (bubbles)

The flow of the discrete phase was simulated with LAG3D code, as has been already explained. Bubbles were entrained in the stirred tank at the bottom, 36 mm away from the shaft and were leaving the tank on the top. The mass flow rate of the gas phase was. It was dictated by the value of gas hold-up in the stirred tank, which could not be bigger than 5% of the tank total volume, in order that the measuring PDA technique used on the experimental setup which served for the validation of the computed results worked properly. Due to such small percentage of the gas in the mixture the coupling of phases was neglected. Flow field parameters were first calculated without using the bubble break-up model and later on using it. This was done in order to estimate the importance of the model inclusion on the accuracy of the calculation.

The inclusion of the break-up model in the computation of the gas phase changed its property fields radically. On fig. 8 the concentration profiles for the stirred tank with the Rushton turbine and for $n = 850$ rot./min. in the vertical cross section exactly between the blades were presented. The inclusion of the break-up model in computation caused much higher bubble concentration in the recirculation zones, which was also visible in the experiments.

For testing the numerical model at the Chair of Fluid Mechanics at the Friedrich Alexander University set of experiments on the stirred tank with Rushton turbine, for both silicon oil and DMSO were performed.

On fig. 9 and fig. 10 the computational and experimental results of the bubble axial velocity in the tank with the Rushton turbine and filled with the silicon oil were presented. The rotational speed was 750 and 850 rot./min. The results for the same geome-

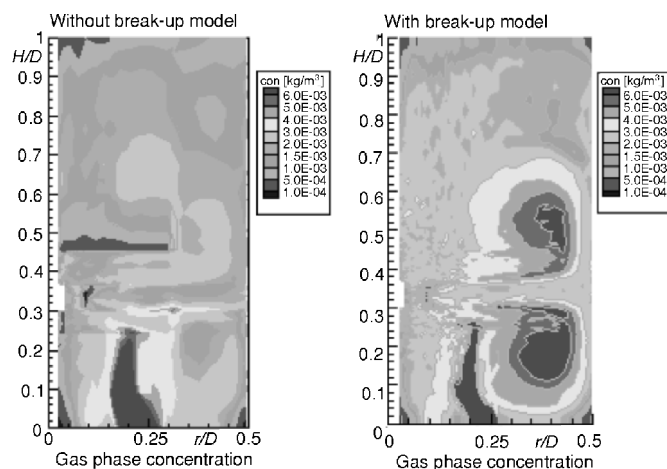


Figure 8. Computed fields of gas phase concentration without using the break-up model (left) and using it (right), $n = 850$ rot./min.

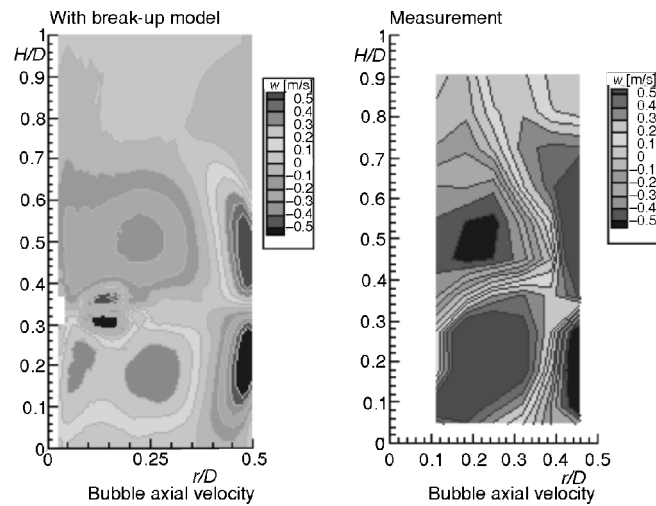


Figure 9. Computed (left) and measured (right) bubble axial velocity profiles for Rushton turbine, $n = 750$ rot./min. (silicon oil)

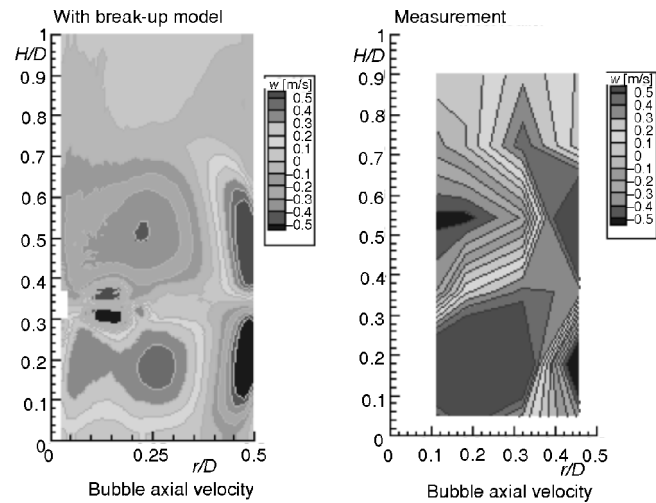


Figure 10. Computed (left) and measured (right) bubble axial velocity profiles for Rushton turbine, $n = 850$ rot./min. (silicon oil)

try but for the DMSO as a liquid and for $n = 650$ rot./min. were presented on fig. 11. Figures represent results in one vertical cross-section. Unfortunately, technical problems throughout the measurements restricted drastically the total number of measured points (in the case of $n = 850$ rot./min. the measurements were performed in only 32 points),

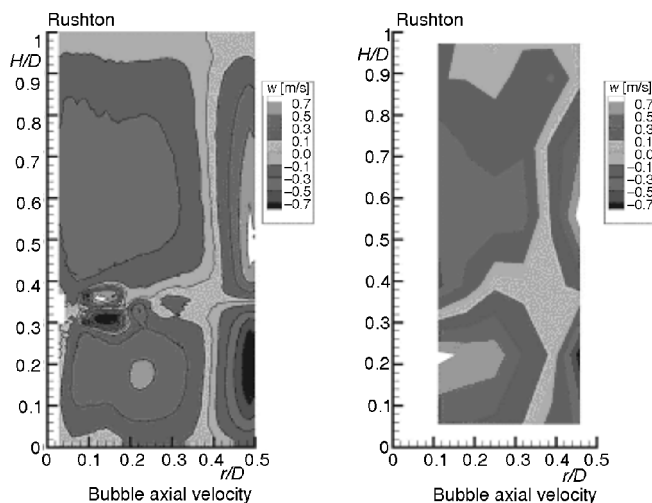


Figure 11. Computed (left) and measured (right) bubble axial velocity profiles for Rushton turbine, $n = 650$ rot./min. (DMSO)

enabling only crude and more qualitative comparison of the computational and experimental results. In this respect it could be said that experiments qualitatively confirmed the computation.

The computed axial velocity profiles of gas phase in the stirred tank with the Pitch blade turbine in both up-flow and down-flow were presented on fig. 12. They are

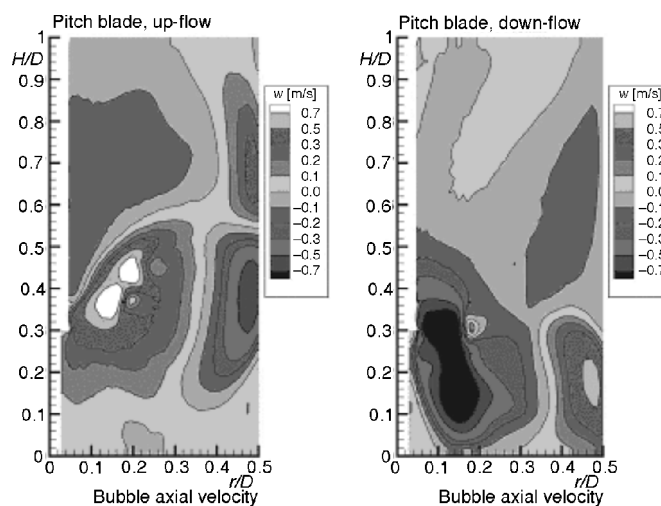


Figure 12. Computed axial velocity profiles of gas phase for Pitch blade turbine for up-flow (left) and down-flow (right), $n = 850$ rot./min. (silicon oil)

very similar to the liquid velocity profiles, fig. 5, which shows the strong dependence of the bubbles trajectories on the liquid velocity profile.

On fig. 13 a computed profiles of bubble concentration for Pitch blade turbine were given. In the case of up-flow motion the higher concentration of gas was obtained in the recirculation zone, compared to the down-flow case. On the other side, down-flow rotation gave much smoother distribution of the gas phase. The explanation for this is more obvious after the insight of average and Sauter bubble diameter distribution, figs. 14 and 15.

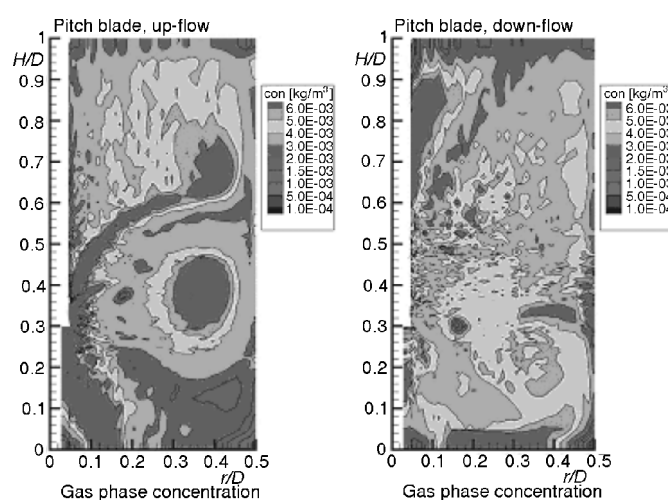


Figure 13. Computed density profiles of gas phase for Pitch blade turbine for up-flow (left) and down-flow (right), $n = 850$ rot./min. (silicon oil)

One can see that both average and Sauter diameter are much smaller in the down-flow case. That could be explained only by the fact that the down-flow rotation keeps bubbles much longer in the stirrer than the up-flow, which has as the consequence that the probability that bubbles pass through the regions of high turbulent kinetic energy becomes bigger, and consequently more bubbles break, giving the smaller average diameter. For smaller bubbles it is becoming now even more difficult to escape, they move randomly through the tank, carried by the liquid, giving more or less average diameter size distribution. In the up-flow big bubbles find their way to the surface much easier do not break so frequently, and since they carry the most of the mass of the gas phase they cause high concentration of the gas phase in the regions through which they pass.

If one compares the values for the average diameter ($d_1 = \Sigma n_i d_i / \Sigma n_i$) and Sauter diameter ($d_{32} = \Sigma n_i d_i^3 / \Sigma n_i d_i^2$) one can realise a big difference in calculated values. That shows that the diameter profiles are very sensitive on the way of diameter averaging. This could be pointed as one of the sources of the difference between computed and

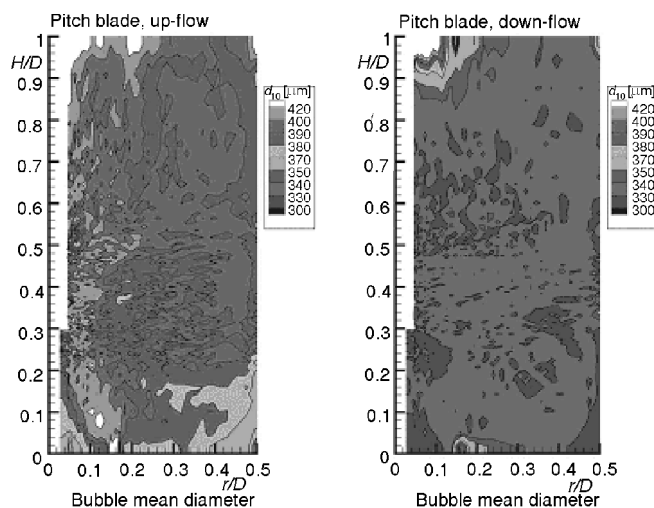


Figure 14. Computed profiles of bubble mean diameter d_{10} for Pitch blade turbine for up-flow (left) and down-flow (right), $n = 850$ rot./min. (silicon oil)

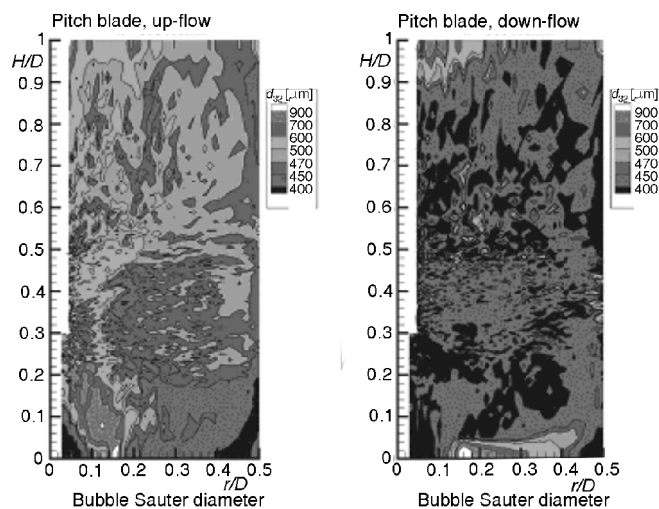


Figure 15. Computed profiles of bubble Sauter diameter d_{32} for Pitch blade turbine for up-flow (left) and down-flow (right), $n = 850$ rot./min. (silicon oil)

measured profiles. In the value of Sauter diameter bigger bubbles which carry most of the mass of the gas phase play more dominant role over the small ones, and consequently this parameter is more relevant in analysis of the physical and chemical processes in the stirrer. In the measurements however, most often one counts bubbles at one point and

calculates average value. Even a good agreement between the measured and calculated average diameter distribution could give wrong gas mass distribution, and opposite. Thus, the differences in the computed and measured profiles of the average diameter do not necessarily mean too big difference in the gas mass distribution.

Conclusion

The inclusion of the break-up model was found necessary for the good simulation of the processes in stirred tanks. A stochastic nature of the occurrence of bubble break-up and sizes of the daughter bubbles was preserved in the model. There exists the value of bubble diameter for which the break-up frequency reaches its maximal value, which is in accordance with the experiments. Small holdup of the gas phase enabled neglect of coupling of phases. Comparison with the experiments showed very good agreement in velocity and concentration profiles of the gas phase. The results for the average bubble diameter are qualitatively the same, but in almost all computations about 20% smaller bubble diameter was got than in the measurements.

Still, some features of the presented model ask for further improvement. The turbulent kinetic energy was introduced indirectly, through the value of turbulent kinetic energy dissipation. It is known that ε much harder to measure, and even in the computation of the single phase fluid flow the obtained field of ε is in many cases not quite accurate. Therefore, even when the break-up model by itself is correct, due to the inaccuracy of the computed ε field the obtained results may not be quite reliable. Also, bubble break-up is connected only with stresses and not with the internal bubble energy which causes instability and break-up. Break-up frequency serves only to determine how often particular bubble breaks. Bubble breaks-up if $\tau_t > \tau_s$. Therefore, the big enough turbulent stress even if it acts only for the short period could cause the break-up, although the total accumulated energy was not necessarily sufficient for this to happen. One way to overcome this inconsistency could be simulation of the bubble energy consumption by the summation of time steps in which $\tau_t > \tau_s$. Bubble would then break-up only when the total accumulated time is greater than t_b *i. e.* the instantaneous bubble break-up time.

Acknowledgment

The financial support of this work through grant Du 101/45-4 from the Deutsche Forschungsgemeinschaft is gratefully acknowledged.

Nomenclature

- B – width of the baffle, m
- D – diameter of the turbine, m
- D_0 – diameter of the mother bubble, m

D_c	– diameter of the smallest bubble which could brake, [m]
D_s, D_b	– diameters of the smaller and bigger daughter bubbles (respectively), [m]
D^*	– non-dimensional diameter, [-]
D_{\min}^*, D_{\max}^*	– minimal and maximal possible non-dimensional diameters, [-]
d_{10}, d_{32}	– average and Sauter diameters, [m]
E_s	– minimal energy necessary to break-up a bubble, [J]
g	– break-up frequency, [s ⁻¹]
H	– height of the water level in the tank, [m]
K_g	– experimentally determined coefficient, [-]
L	– distance between the acting points of turbulent stresses, [m]
L_{\min}	– distance between the turbulent stresses necessary to break-up a bubble, [m]
n	– angular velocity, [rot./min.]
$P(L), P(D^*)$	– p.d.f. of L and D^* , [-]
Re	– Reynolds number, [-]
r	– radial position, [m]
T	– Tank diameter, [m]
t	– time, [s]
t_b	– break-up time, [s]
u	– velocity of fluid, [m/s]
w	– component of axial velocity, [m/s]
x	– position, [m]

Greek letters

β	– Batchelor coefficient, [-]
Δ	– finite difference, [-]
ε	– dissipation of turbulent kinetic energy, [m ² s ⁻³]
ρ	– density, [kgm ⁻³]
σ	– surface tension, [Nm ⁻¹]
τ_t, τ_s	– turbulent and restoring stresses (respectively), [Nm ⁻²]

References

- [1] Batchelor, G. K., The Theory of Homogenous Turbulence, Cambridge University Press, Cambridge, UK, 1956
- [2] Brenn, G., Braeske, H., Živković, G., Durst, F., Experimental and Numerical Investigation of Liquid Channel Flows with Dispersed Gas and Solid Particles, *Int. J. Multiphase Flow*, 29 (2003), pp. 219-247
- [3] Crowe, C. T., Sharma, M. P., Stock, D. E., The Particle-Source-in-Cell (PSI-CELL) Model for Gas-Droplet Flows, *J. Fluids Eng.* 99 (1977), 99, pp. 325-332
- [4] Martinez-Bazan C., Montanes, J. L., Lasheras, J. C., On the Breakup of an Air Bubble Injected into a Fully Developed Turbulent Flow, Part 1, Breakup Frequency, *J. Fluid Mech.* 401 (1999), pp. 157-182
- [5] Martinez-Bazan, C., Montanes, J. L., Lasheras, J. C., On the Breakup of an Air Bubble Injected into a Fully Developed Turbulent Flow, Part 2, Size PDF on the Resulting Daughter Bubbles, *J. Fluid Mech.* 401 (1999), pp. 183-207
- [6] Matsumoto, S., Saito, S., Monte Carlo Simulation of Horizontal Pneumatic Conveying Based on the Rough Wall Model, *J. Chem. Engng. Japan*, 3 (1970), pp. 223-230

- [7] Migdal, D., Agosta, V. D., A Source Flow Model for Continuum Gas-Particle Flow, *Trans. ASME*, 34 (1967), pp. 860-865
- [8] Milojević, D., Lagrangian Stochastic-Deterministic (LSD) Prediction of Particle Dispersion in Turbulence, *Part. Part. Syst. Charact.* 7 (1990), pp. 181-190
- [9] Mostafa, A. A., Elghobashi, S. E., A Two-Equation Turbulence Model for JET Flows Laden with Vaporising Droplets, *Int. J. Multiphase Flow*, 11 (1985), pp. 515-533
- [10] Oesterle, B., Petitjean, A., Simulation of Particle-to-Particle Interaction in Gas-Solid Flows, *Int. J. Multiphase Flow*, 19 (1993), pp. 199-211
- [11] Rubinow, S. I., Keller, B., The Transverse Force on a Spinning Sphere Moving in a Viscous Fluid, *J. Fluid Mech.*, 11 (1961), pp. 447-459
- [12] Saffman, P. G., The Lift on a Small Sphere in a Shear Flow. *J. Fluid Mech.*, 22 (1965), pp. 385-400
- [13] Schäfer, M., Höfken, M., Durst, F., Detailed LDV Measurements for Visualization of the Flow Field within a Stirred-Tank Reactor Equipped with a Rushton Turbine, *Trans. IChemE*, 75(A) (1997), pp. 729-736
- [14] Sommerfeld, M., Živković, G., Recent Advances in the Numerical Simulation of Pneumatic Conveying through Pipe Systems, *Proceedings, Computational Methods in Applied Science, Invited Lectures and Special Technological Sessions of the 1st European Computational Fluid Dynamics Conference*, Brussels, 1992, pp. 201-212
- [15] Tsuji, Y., Oshima, T., Morikawa, Y., Numerical Simulation of Pneumatic Conveying in a Horizontal Pipe, *KONA*, 3 (1985), pp. 38-51
- [16] Wechsler, K., Breuer, M., Durst, F., Steady and Unsteady Computations of Turbulent Flows Induced by a 4/45° Pitched Blade Impeller, *Journal of Fluids Engineering*, 121 (1999), pp. 318-329

Author's address:

G. Živković, S. Nemoda
VINČA Institute for Nuclear Sciences
Laboratory for Thermal Engineering and Energy
P. O. Box 522, 11001 Belgrade
Serbia and Montenegro

Corresponding author (G. Živković):
Phone: ++38111/11/2458222 ext.279
Fax: ++38111/11/453670
E-mail: gzivkovi@vin.bg.ac.yu

Paper submitted: February 5, 2004
Paper revised: March 18, 2004
Paper accepted: April 23, 2004